HHS Public Access

Author manuscript

Hum Mutat. Author manuscript; available in PMC 2017 May 01.

Published in final edited form as:

Hum Mutat. 2016 May ; 37(5): 481–487. doi:10.1002/humu.22961.

MYO3A causes human dominant deafness and interacts with protocadherin 15-CD2 isoform

M'hamed Grati[1,#], **Denise Yan**[1], **Manmeet H. Raval**[2], **Tom Walsh**[3], **Qi Ma**[1], **Imen Chakchouk**[1,4], **Abhiraami Kannan-Sundhari**[1], **Rahul Mittal**[1], **Saber Masmoudi**[4], **Susan H. Blanton**[1,5], **Mustafa Tekin**[1,5], **Mary-Claire King**[3], **Christopher M. Yengo**[2], and **Xue Zhong Liu**[1,5,6,#]

[1] Department of Otolaryngology, University of Miami Miller School of Medicine, Miami, FL 33136, USA

[2] Department of Cellular and Molecular Physiology, Pennsylvania State University College of Medicine, Hershey, Pennsylvania 17033

[3] Departments of Medicine and Genome Sciences, University of Washington, Seattle, WA, 98195-7720, USA

[4] Laboratoire Procédés de Criblage Moléculaire et Cellulaire, Centre de Biotechnologie de Sfax, Université de Sfax, Sfax, Tunisie

[5] Dr. John T. Macdonald Foundation, Department of Human Genetics, and John P. Hussman Institute for Human Genomics, University of Miami, Miami, FL 33146, USA

[6] Department of Otolaryngology, Xiangya Hospital, Central South University, Changsha, Hunan, China

Abstract

Hereditary hearing loss is characterized by both allelic and locus genetic heterogeneity. Both recessive and dominant forms of hearing loss may be caused by different mutations in the same deafness gene. In a family with post-lingual progressive non-syndromic deafness, whole exome sequencing of genomic DNA from five hearing-impaired relatives revealed a single variant, p.Gly488Glu (rs145970949:G>A) in *MYO3A*, co-segregating with hearing loss as an autosomal dominant trait. This amino acid change, predicted to be pathogenic, alters a highly conserved residue in the motor domain of MYO3A. The mutation severely alters the ATPase activity and motility of the protein *in vitro*, and the mutant protein fails to accumulate in the filopodia tips in COS7 cells. However, the mutant MYO3A was able to reach the tips of organotypic inner ear

[#]**Correspondence to:** Prof. Xue Zhong Liu, Department of Otolaryngology (D-48), University of Miami, 1666 NW 12th Avenue, Miami, Florida 33136, USA, xliu@med.miami.edu, Tel: 305 243 1484; Fax: 305 243 2009. [#]Prof. M'hamed Grati, Department of Otolaryngology (D-48), University of Miami, 1601 NW 12th Avenue, Miami, Florida 33136, USA, m.grati@med.miami.edu, Tel: 305 243 4923; Fax: 305 243 4925.

Author's contribution

M.G., D.Y., M.H.R., T.W., M.-C.K., C.M.Y. and X.Z.L. designed research; M.G., D.Y., M.H.R., T.W., Q.M., I.C., A.K.-S. and R.M. performed research; M.G., D.Y., M.H.R., T.W., I.C., M.-C.K., C.M.Y. and X.Z.L. analyzed the data; M.G. wrote the paper; M.G., D.Y., M.H.R., T.W., S.M., S.H.B., M.T., M.-C.K., C.M.Y. and X.Z.L. edited the paper.

Competing financial interests

The authors declare no competing financial interests.

culture hair cell stereocilia, raising the possibility of a local effect on positioning of the mechano-electrical transduction (MET) complex at the stereocilia tips. To address this hypothesis, we investigated the interaction of MYO3A with the cytosolic tail of the integral tip-link protein protocadherin 15 (PCDH15), a core component of MET complex. Interestingly, we uncovered a novel interaction between MYO3A and PCDH15 shedding new light on the function of myosin IIIA at stereocilia tips.

Keywords

Dominant Autosomal Deafness; MYO3A; Protocadherin 15-CD2; Ear Sensory Hair Cells; Mechanotransduction Complex

Introduction

Genome wide exome capture and NextGen deep sequencing have revolutionized the field of genetic hearing loss by accelerating the discovery of novel hearing loss (HL) -causing genes [Yan et al., 2013; Shearer et al., 2011; Avraham & Kanaan, 2012]. To date, more than 80 genes have been identified to cause non-syndromic HL (http://hereditaryhearingloss.org/) with most of them being identified through linkage analysis in large pedigrees and positional gene cloning, combined in cases with candidate gene approach (example, [Yasunaga et al., 1999]). The NextGen approach has proven successful and is increasingly important in identifying HL genes within small families [Walsh et al., 2010; Pierce et al., 2010 and 2011; Sirmaci et al., 2012].

Mutations in *MYO3A* (MIM# 606808) cause nonsyndromic recessive progressive HL (DFNB30) [Walsh et al., 2002] and a mouse model exhibits significant HL beginning at high frequencies and eventually progressing to all frequencies [Walsh et al., 2011]. Class III myosins consist of two homologous myosins (a and b) composed of an N-terminal regulatory kinase domain, a motor-head domain, and a characteristic C-terminal tail comprising an N-terminal unit (3THD-I) that binds the Ankyrin-repeat domain of the long form of espin (Espin-1) and an additional C-terminal domain (3THD-II) that is present only in myosin IIIa and binds to actin [Salles et al., 2009]. These two myosins are suspected to play partially redundant roles in inner ear sensory hair cells (HC; [Manor et al., 2012]). Only deleterious recessive mutations in MYO3A have so far been identified leading to a form of late onset progressive HL in human [Walsh et al., 2002].

In this study, we report an amino acid substitution in MYO3A motor-head domain that can cause autosomal dominant progressive HL. We demonstrate in vitro that this mutation alters the ATPase activity of Myosin IIIa (MYO3A) that would alter its local function at the HC stereocilia tips. We also revealed a novel interaction of MYO3A with the protocadherin15 (PCDH15) CD2 isoform cytosolic tail that would directly implicate MYO3A in mechanotransduction (MET).

Materials and Methods

Subjects and Clinical Evaluations

This study was approved by institutional review boards (IRB) of the University of Miami. Written informed consent was obtained from adult subjects and the parents of minor subjects. Clinical history interviews and physical examinations of members of the family ruled out the implication of environmental factors for causing the hearing loss and the presence of a syndrome in the father and three children. The degree of hearing impairment was assessed by pure audiometry test that was performed to test air conduction and bone conduction at frequencies ranging from 250 to 8,000 Hz. Peripheral blood samples were collected from participant subjects for genomic DNA extraction following phenol-chloroform method. Details on subject ascertainment were described in King et al. [2012].

GenBank Accession Numbers

Protein: NP_059129.3; mRNA: NM_017433.4.

Complementary DNA Constructs, immunocytochemistry, imaging and fluorescence quantifications

Plasmid construct encoding for N-terminally Cherry-tagged human Myosin IIIA deleted of its kinase domain (Ch-MYO3A-ΔK) has been described in Quintero et al. [2010]. Plasmid construct encoding Gly488Glu point mutated Ch-MYO3A-ΔK was generated using QuickChange II XL Site Directed Mutagenesis Kit (Agilent Technologies). Clones obtained were fully sequenced and correct mutated clones were isolated and plasmid DNA preparations were made. Plasmid construct encoding untagged espin1 (long form of espin) has been used in Salles et al. [2009]. Plasmid construct encoding for N-terminally GFP-tagged mouse Myosin IIIB deleted of its kinase domain (Ch-Myo3b-ΔK) has been described in Merritt et al. [2012]. Chimeric fusion between cDNA encoding mouse pcdh15-CD2.1 cytosolic tail (amino acid sequence 1410-1790 of NP_001136214) and cDNA encoding plasma membrane IL2RA/CD25 (TAC) was generated in pcDNA3 expression vector (Invitrogen, CA; used in Grati et al., [2006]) using standard PCR methods. Tac was revealed using mouse antibody purchased from Novus Biologicals (catalog# NB600-564). Immunocytochemistry was performed on COS7 cells as described in Grati & Kachar [2011]. Images were taken on a LSM710 confocal microscope equipped with a 63x 1.4 numerical aperture (N.A.) objective (Zeiss Microimaging). Confocal images were processed using Adobe photoshop, and NIH ImageJ was used for fluorescence quantifications. Relative pixel intensity of fluorescently tagged proteins (on individual channels) along selected filopodia was determined using “Plot profile” analysis tool in NIH ImageJ software. ImageJ user guide can be found at “imagej.nih.gov/ij/docs/guide/user-guide.pdf”.

The baculovirus system was used to express human MYO3A constructs (pFBMYO3AΔK2IQ c-GFP WT and pFBMYO3A ΔK 2IQ c-GFP G488E) that lacked the kinase domain and were truncated after the second IQ domain (aa340-805) of NM_017433.4 (containing naturally occurring variants I348V and V369I; [Greenman et al., 2007]). Both constructs contain a COOH-terminal GFP followed by a FLAG tag. The pFBMYO3AΔK2IQ WT, without the c-GFP was described previously [Dosé et al., 2008].

The G488E point mutation was inserted using QuickChange II XL Site Directed Mutagenesis Kit (Agilent Technologies).

Actin-activated ATPase Activity and In vitro motility Assays. The actin-activated ATPase activity was performed by utilizing the NADH coupled assay in the presence of 1 mM ATP in KMg50 Buffer (10 mM Imidazole, 50 mM KCl, 1 mM $MgCl_2$, 1 mM EGTA, 1 mM DTT) [Dosé et al., 2007; Dosé et al., 2008; Quintero et al., 2010]. The concentration of MYO3AΔK2IQ c-GFP purified by anti-FLAG immunoaffinity chromatography was determined with gel densitometry using MYO3A2IQ [Dosé et al., 2007] as a standard. The Michaelis-Menten equation was used to determine the k_{cat} (maximal actin-activated ATPase rate) and K_{ATPase} (actin concentration at which the ATPase activity is one-half maximal) using a hyperbolic fit of the ATPase rates as a function of actin concentration. The in vitro motility assay was performed as described [Trivedi et al., 2013, Yengo et al., 2012]. Briefly, WT or G488E MYO3A ΔK 2IQ c-GFP were attached to the nitrocellulose-coated glass coverslip surface using an anti-GFP antibody (Life Technologies) and the surface was then blocked with 1mg/mL BSA solution in KMg50 buffer. The activation buffer consisted of KMg50 supplemented with 0.35% methylcellulose, 10 μM calmodulin, 1mg/mL BSA, 2 mM ATP, and 20 units/mL pyruvate kinase and 2.5mM phosphoenol pyruvate were added as an ATP regeneration system. To reduce photobleaching 1mg/mL glucose, 0.1mg/mL glucose oxidase and catalase were also added. Finally, after the addition of activation buffer, the motility of the rhodamine-phalloidin labeled F-actin filaments was observed using Nikon TE2000 microscope. The time-lapse images were acquired at 5s intervals for a period of 10 minutes. The velocity of moving actin filaments was measured using ImageJ (with MtrackJ plugin) [Meijering et al., 2012].

Whole Exome Sequencing, Mutation Analysis and SNPs Genotyping by Sanger Sequencing on Genomic DNA, Animal Use, and Helios Gene Gun Transfections

Detailed protocols can be found in Supp. Methods.

Results

A missense mutation in MYO3A causes autosomal dominant sensorineural hearing loss in an African-American family

The family subject of this study is a two-generational African-American kindred with hearing loss in both parents and all three children, with onset in the early childhood and significant progression (Fig. 1A). All three 5-9 year old siblings had bilateral early onset post-lingual moderate HL (Fig. 1A), while their 46-year-old father had profound bilateral HL (Fig. 1A), showing the progressive loss by history. Bone conduction thresholds excluded conductive hearing impairment, and clinical examination was negative for any findings consistent with syndromic HL. No family history of HL was reported from both parent sides.

Exome sequencing was performed on all 5 family members with an average depth of coverage of 110x, as described in Walsh et al. [2010]. Exome variants were initially filtered to identify genes that: (i) harbored potentially damaging (PolyPhen > 0.8, GERP > 5.0), (ii) were rare (less than 0.01 MAF in African Americans) and (iii) homozygous or compound

heterozygous in all three children. However, no genes remained after these filters were applied. Filtering to three-way shared variants that were heterozygous and rare and potentially damaging, inherited from either parent yielded just one variant: NC_000010.10:g.26377235G>A (Fig. 1A, C) corresponding to c.1463G>A (p.Gly488Glu; rs145970949:G>A) in MYO3A, inherited from the father. The variant was supported by the following read depth (variant/total reads): 14/26 in the Father, 23/55 in the Son, 25/53 in 1st Daughter and 20/42 in the 2nd Daughter, and was absent from the Mother. All 5 family members were Sanger sequenced at this location to confirm the exome genotypes. The mutation occurs in a highly conserved residue in the myosin motor (Fig. 1D) located in the switch I region (Fig. 1B, D). The p.Gly488Glu variant has been predicted to be highly damaging (Mutation Taster P=0.99; Polyphen-2 score 1.00). On ExAC server (http://exac.broadinstitute.org/), this variant was found heterozygote in 7 of 5,133 Africans (10,266 chromosomes), for an allele frequency of 0.0007, and in 2 of 5,782 Latinos (11,564 chromosomes), for an allele frequency of 0.0002; the hearing phenotype of all career individuals found on ExAC server is unknown. This variant has not been found in other populations.

We also studied the maternal *MYO3A* allele inheritance into children by SNP genotyping and haplotype segregation analysis (Fig. 1A). All three children were found not to inherit the same maternal SNP haplotypes and therefore inherited distinct maternal *MYO3A* alleles.

Characterization of the effect of p.Gly488Glu mutation on MYO3A ATPase activity and motility *in vitro*

We examined the impact of the p.Gly488Glu mutation on the enzymatic and motile properties of MYO3A using actin-activated ATPase and *in vitro* motility assays, respectively. We expressed and purified wild-type and mutant MYO3A lacking the kinase domain and containing the motor and 2IQ domains as well as a COOH-terminal GFP tag. The FLAF –affinity purified mutant and wild-type GFP-tagged MYO3A were examined by Coomassie stained SDS-PAGE gels and found to be of similar purity (~60% pure). A band of the correct molecular weight (119803 kDa, corresponding to the MYO3A heavy chain) was identified by Western blot using anti-GFP antibody. The p.Gly488Glu mutation reduced the maximal actin-activated ATPase activity (K_{cat}; Fig. 2C) and increased the actin concentration required for reaching one-half maximal ATPase activity (K_{ATPase}; Fig. 2A, C). In the *in vitro* motility assay, we utilized the COOH-terminal GFP tag to adhere MYO3A to the nitrocellulose cover slip. We examined the actin sliding velocity with both mutant and wild-type MYO3A. Interestingly, the mutant MYO3A displayed a two-fold enhanced actin filament sliding velocity compared to the wild type (Fig. 2B, C). Overall, the enzymatic and motor characterization of the p.Gly488Glu mutation demonstrates this mutation reduces actin affinity and enhances sliding velocity, which suggests an enhanced ADP release rate constant [Yengo et al., 2012].

Characterization of the effect of p.Gly488Glu mutation on MYO3A localization in hair cells

We examined the transport and localization of mutant Ch-MYO3A-ΔK p.Gly488Glu in organotypic rat inner ear culture hair cells. Ch-MYO3A-ΔK p.Gly488Glu was able to reach and accumulate into the stereocilia tips (Fig. 2D) at similar levels and localization pattern as

we have previously observed with wild type GFP-MYO3A-ΔK [Quintero et al., 2010]. Mutant Ch-MYO3A-ΔK p.Gly488Glu accumulated in stereocilia tips in a reverse gradient with stereocilia length, similar to what we have previously seen with wild type GFP-MYO3A-ΔK [Quintero et al., 2010].

Characterization of the effect of p.Gly488Glu mutation on MYO3A localization in COS7 cells

We tested the effect of the p.Gly488Glu mutation on MYO3A localization and transport activity of its known cargo Espin1 in COS7 cells. As has been shown, wild type MYO3A induces filopodial actin protrusions and localizes to their tips, particularly well when its kinase domain was removed ([Salles et al., 2009]; Fig. 3A), since its kinase activity autoregulates its motility, transport, filopodia tip accumulation rate, and actin bundle formation and stability [Quintero et al., 2010; Quintero et al., 2013]. In all our experiments, we used a construct encoding for Cherry-tagged MYO3A containing the p.Gly488Glu mutation lacking its kinase domain (Ch-MYO3A-ΔK p.Gly488Glu) to accurately visualize the impact of the p.Gly488Glu mutation on motility and filopodia tip accumulation while eliminating any interference of autophosphorylation events on its filopodia transport rate. We found that Ch-MYO3A-ΔK p.Gly488Glu failed to accumulate to filopodia tips (Fig. 3B), or to elongate filopodia in the presence of Espin1 (Fig. 3D) compared to wild type Ch-MYO3A-ΔK (Fig. 3C). Mutant Ch-MYO3A-ΔK p.Gly488Glu was however found randomly present within the cytosol (Fig. 3B), or abundantly bound to Espin1-bundled actin cables (Fig. 3D). Co-expression of wild type GFP-MYO3A-ΔK together with mutant Ch-MYO3A-ΔK p.Gly488Glu and Espin1 did not lead to the transport-accumulation of the Ch-MYO3A-ΔK p.Gly488Glu at the filopodia tips, whereas wild type GFP-MYO3A-ΔK localization to filopodia tips was unperturbed (Fig. 3E).

Identification of protocadherin 15 CD2 isoform as new cargo/ligand for MYO3A

Protocadherin 15 (PCDH15) isoforms are essential components of developing stereocilia lateral and form tip links, as well as stereocilia-kinocilia links. Particularly, the PCDH15 CD2 isoform (PCDH15-CD2) has been shown as an essential component of the lower tip-link density (at the tips of stereocilia) in mature auditory hair cells [Pepermans et al., 2014]; the MET complex that is formed of several known and many more unknown proteins, is located at the lower tip-link density. Therefore, we investigated in COS7 cells the interaction of MYO3A with the PCDH15-CD2 cytosolic tail fused to a reporter plasma membrane protein, the Interleukin 2-α receptor (Tac). We observed that Ch-MYO3A-ΔK efficiently carries and accumulates Tac-CD2 fusion protein to the tips of filopodia (Supp. Fig. S1A). In the presence of Espin1, Ch-Myo3A-ΔK was able to elongate filopodia, carry and accumulate Espin1 into filopodia tips, and also carries and accumulates Tac-CD2 to all filopodia tips (Supp. Fig. S1B, C). However, Tac alone was not carried and therefore not accumulated to filopodia tips (Supp. Fig. S1D). Ch-MYO3A-ΔK p.Gly488Glu was not able to carry either of Tac-CD2 (Supp. Fig. S1E), Espin1 (Supp. Fig. S1E, F) or Tac (Supp. Fig. S1F) to filopodia, or to elongate filopodia (Supp. Fig. S1E, F).

Protocadherin15 CD2 is not a Myo3b cargo/ligand

We investigated in COS7 cells whether CD2 is a Myo3b cargo/ligand. We used Ch-Myo3b-ΔK that we previously demonstrated binds to Espin1 for motility and carries it to the tip portion of COS7 cell filopodia, leading to filopodia extention [Merritt et al., 2012]. Coexpression of Ch-Myo3b-ΔK, GFP-Espin1 and Tac (fused or not to CD2 cytosolic tail) resulted in a fluorescence profile that after quantification demonstrated Ch-Myo3b-ΔK was able to carry GFP-Espin1 to filopodia tips leading to filopodia elongation. Their colocalized fluorescence co-distribute in a rod like shape starting at the filopodia tips (Supp. Fig. S2A, B). However, neither the Tac (Supp. Fig. S2B) or Tac-CD2 (Supp. Fig. S2A) respective fluorescence intensity profiles along the filopodia coincided with that of the Ch-Myo3b-ΔK::GFP-Espin1 complex within this subcellular region (Supp. Fig. S2). Tac and Tac-CD2 fluorescence intensity profile was however constant along the filopodia and very comparable to that observed in the rest of the plasma membrane outside filopodia (Supp. Fig. S2).

Discussion

Mutations in several unconventional myosins cause human deafness [Duman and Tekin, 2012]. They play crucial distinct roles in the development, maturation and operation of hair cell (HC) stereocilia hair bundle-mediated mechanotransduction (MET) and are found to define distinct subcellular compartments [Schneider et al., 2006]. Myosin VIIa, as part of the Usher type 1 network, orchestrates the early developmental organization of the stereocilia hair bundle, and likely mediates tip-link tension in mature HCs [Grati & Kachar, 2011]. Recently, a longer splice isoform of Myosin XVa was shown to localize to the lower tip-link density [Fang et al., 2015], similarly to PCDH15-CD2. Myosin XVa is implicated in stereocilia length regulation by monitoring the transport of EPS8 and Whirlin to stereocilia tips [Manor et al., 2011]. Myosin Ic likely anchors the apical stereocilia plasma membrane to its adjacent stereocilia actin core [Schneider et al., 2006]. Myosin VI plays an important role in anchoring the stereocilia actin tapered-base and the cuticular plate actin network to their adjacent plasma membranes [Self et al., 1999; Seiler et al., 2004]. However, the function of stereocilia class III myosins is still poorly understood. In particular, myosin IIIa (MYO3A) is highly expressed in sensory hair cells and localizes abundantly to the tips of mechanosensory stereocilia in a thimble-like distribution [Schneider et al., 2006]. Human MYO3A deleterious mutations cause recessive sensory deafness [Walsh et al., 2002] which implies that MYO3A plays important role in hair cell function. Early investigations led us to assume that MYO3A is a cargo transporter to stereocilia tips [Salles et al., 2009]. Mouse knock-in of the most severe human deleterious mutation shed light about Myosin IIIA pathophysiology [Walsh et al., 2011].

Here we uncovered a dominant mutation in MYO3A motor-head domain that is the most likely and unique cause of progressive moderate to severe hearing loss in 4 members of an African-American family. The father of this family with deafness transmitted a p.Gly488Glu variant to all three of his children. Moreover, all three children were found not to inherit the same maternal *MYO3A* locus-covering SNP haplotype, ruling out the possibility of their inheritance of a second uncovered maternal mutant allele that would be in *MYO3A* non-coding regions, and further corroborating our finding of their paternal inheritance of the only

MYO3A c.1463G>A mutant allele. We show that this mutation reduces the *in vitro* ATPase activity of MYO3A but enhances its motility. Thus, the mutation is not simply a motor-dead mutation. Interestingly, in COS7 cells, we found that the mutation abolished the filopodial-tip accumulation of the protein. Surprisingly, tagged mutated MYO3A was found capable of reaching the tips of rat organotypic inner ear culture hair cell stereocilia, and showed a fluorescence pattern similar to that seen for wild type MYO3A [Schneider et al., 2006; Salles et al., 2009]. We propose that although this mutant form of MYO3A is capable of generating actin sliding in an ensemble-based motility assay, its ability to walk as an inchworm along actin bundles may be severely impaired. This may be the case if the mutation alters the MYO3A ATPase cycle in such a way such that it would disrupt the walking mechanism of this motor. For example, the mutation may alter the duty ratio, the fraction of the ATPase cycle that the myosin is strongly bound to actin. Alternatively, the mutation might disrupt the coordination between the motor and tail actin binding sites. The duty ratio and moto-tail coordination may be crucial for MYO3A movement in the filopodia of COS7 cells, while the movement in stereocilia may involve a complex of MYO3A and/or other actin-based motors.

In this study, our proposed mechanism raises the possibility of passive transport of this mutated version in cultured hair cells either i) independently from the endogenously expressed wild type MYO3A, or also ii) in association with the endogenously expressed wild type MYO3A, in case where unknown hair cell specific ligand would allow MYO3A oligomerization. Consequently, we speculate that in order for the mutated MYO3A to cause deafness, it would exert a local dominant effect on the MET complex at the stereocilia tips. Our investigations of direct association of MYO3A with a key protein of MET complex, protocadherin 15 (PCDH15), revealed a novel interaction between MYO3A and the cytosolic tail of PCDH15-CD2 isoform, which is the lower tip-link integral protein in mature auditory hair cells [Kazmierczak et al., 2007; Pepermans et al., 2014]. We found MYO3A transports PCDH15-CD2 to the tips of filopodia. Our results also suggest that Myo3b is unable to target/transport TAC-CD2 to actin protrusion tips, indicating a specific, non-overlapping role for MYO3A. Biochemical data and a close examination of the ultrastructure of the tip-link showed that Protocadherin 15 forms a homodimer [Kazmierczak et al., 2007]. These observations together with our findings leads us to speculate that during the transport of PCDH15 dimers across hair cell stereocilia towards their tips, either as a cargo of wild type MYO3A or via other molecular motors, such as Myosin VIIa [Senften et al., 2006] or Myosin XVa [Fang et al., 2015], mutated MYO3A could be carried passively to stereocilia tips bound to PCDH15 cytosolic tail and thereby accumulates at stereocilia tips, as observed in our experiments. This possible mechanism implies that wild type and mutant MYO3A may also form a heterogeneous cluster at stereocilia tips that would be directly associated with the MET complex via PCDH15-CD2.

In the present model, MYO3A plays a crucial role in positioning the MET complex in coordination with stereocilia actin core elongation during the development of the hair bundle, as well as during its maintenance after maturation. The accumulation of mutant MYO3A through time would worsen MET dysfunction and therefore increase the severity of deafness, as observed when comparing the audiometry evaluations of 5-9 years old children and their 46 year-old father (Fig. 1A).

Overall, our findings shed a new light on the role of MYO3A in MET. Further investigations of hair cells MET physiological properties in a p.Gly488Glu mouse knock-in model would better clarify the function of Myo3a in relation to the MET complex.

Supplementary Material

Refer to Web version on PubMed Central for supplementary material.

Acknowledgments

We gratefully thank all the subjects in this study for their collaboration. We thank Dr. Uri Manor (National Institutes of Health) for his critical reading and input on the manuscript.

Grant Sponsors: This study was supported by the National Institutes of Health grants R01DC005575, R01DC012115 and R01DC012546 to X.Z.L., The American Hearing Research Foundation grant to M.G., R01DC009645 to M.T., and the Pennsylvania Lions Hearing Research Foundation to C.M.Y.

References

Avraham KB, Kanaan M. Genomic advances for gene discovery in hereditary hearing loss. J Basic Clin Physiol Pharmacol. 2012; 23(3):93–97. [PubMed: 22962211]

Dosé AC, Ananthanarayanan S, Moore JE, Burnside B, Yengo CM. Kinetic mechanism of human myosin IIIA. J Biol Chem. 2007; 282(1):216–231. [PubMed: 17074769]

Dosé AC, Ananthanarayanan S, Moore JE, Corsa AC, Burnside B, Yengo CM. The kinase domain alters the kinetic properties of the myosin IIIA motor. Biochemistry. 2008; 47(8):2485–2496. [PubMed: 18229949]

Duman D, Tekin M. Autosomal recessive nonsyndromic deafness genes: a review. Front Biosci. 2012; 17:2213–2236.

Fang Q, Indzhykulian AA, Mustapha M, Riordan GP, Dolan DF, Friedman TB, Belyantseva IA, Frolenkov GI, Camper SA, Bird JE. The 133-kDa N-terminal domain enables myosin 15 to maintain mechanotransducing stereocilia and is essential for hearing. Elife. 2015:4. doi: 10.7554/eLife.08627.

Grati M, Aggarwal N, Strehler EE, Wenthold RJ. Molecular determinants for differential membrane trafficking of PMCA1 and PMCA2 in mammalian hair cells. J Cell Sci. 2006; 119:2995–3007. Pt 14. [PubMed: 16803870]

Grati M, Kachar B. Myosin VIIa and sans localization at stereocilia upper tip-link density implicates these Usher syndrome proteins in mechanotransduction. Proc Natl Acad Sci U S A. 2011; 108(28): 11476–11481. [PubMed: 21709241]

Greenman C, Stephens P, Smith R, Dalgliesh GL, Hunter C, Bignell G, Davies H, Teague J, Butler A, Stevens C, Edkins S, O'Meara S, et al. Patterns of somatic mutation in human cancer genomes. Nature. 2007; 446(7132):153–158. [PubMed: 17344846]

Kazmierczak P, Sakaguchi H, Tokita J, Wilson-Kubalek EM, Milligan RA, Müller U, Kachar B. Cadherin 23 and protocadherin 15 interact to form tip-link filaments in sensory hair cells. Nature. 2007; 449(7158):87–91. [PubMed: 17805295]

King PJ, Ouyang X, Du L, Yan D, Angeli SI, Liu XZ. Etiologic diagnosis of nonsyndromic genetic hearing loss in adult vs pediatric populations. Otolaryngol Head Neck Surg. 2012; 147(5):932–936. [PubMed: 22785241]

Manor U, Disanza A, Grati M, Andrade L, Lin H, Di Fiore PP, Scita G, Kachar B. Regulation of stereocilia length by myosin XVa and whirlin depends on the actin-regulatory protein Eps8. Curr Biol. 2011; 21(2):167–172. [PubMed: 21236676]

Manor U, Grati M, Yengo CM, Kachar B, Gov NS. Competition and compensation: Dissecting the biophysical and functional differences between the class 3 myosin paralogs, myosins 3a and 3b. Bioarchitecture. 2012; 2(5):171–174. [PubMed: 22954581]

Mecklenburg KL, Freed SA, Raval M, Quintero OA, Yengo CM, O'Tousa JE. Invertebrate and vertebrate class III myosins interact with MORN repeat-containing adaptor proteins. PLoS One. 2015; 10(3):e0122502. [PubMed: 25822849]

Meijering E, Dzyubachyk O, Smal I. Methods for cell and particle tracking. Methods Enzymol. 2012; 504:183–200. [PubMed: 22264535]

Merritt RC, Manor U, Salles FT, Grati M, Dose AC, Unrath WC, Quintero OA, Yengo CM, Kachar B. Myosin IIIB uses an actin-binding motif in its espin-1 cargo to reach the tips of actin protrusions. Curr Biol. 2012; 22(4):320–325. [PubMed: 22264607]

Pepermans E, Michel V, Goodyear R, Bonnet C, Abdi S, Dupont T, Gherbi S, Holder M, Makrelouf M, Hardelin JP, Marlin S, Zenati A, Richardson G, Avan P, Bahloul A, Petit C. The CD2 isoform of protocadherin-15 is an essential component of the tip-link complex in mature auditory hair cells. EMBO Mol Med. 2014; 6(7):984–992. [PubMed: 24940003]

Pierce SB, Walsh T, Chisholm KM, Lee MK, Thornton AM, Fiumara A, Opitz JM, Levy-Lahad E, Klevit RE, King MC. Mutations in the DBP-deficiency protein HSD17B4 cause ovarian dysgenesis, hearing loss, and ataxia of Perrault Syndrome. Am J Hum Genet. 2010; 87(2):282–288. [PubMed: 20673864]

Pierce SB, Chisholm KM, Lynch ED, Lee MK, Walsh T, Opitz JM, Li W, Klevit RE, King MC. Mutations in mitochondrial histidyl tRNA synthetase HARS2 cause ovarian dysgenesis and sensorineural hearing loss of Perrault syndrome. Proc Natl Acad Sci U S A. 2011; 108(16):6543–6548. [PubMed: 21464306]

Quintero OA, Moore JE, Unrath WC, Manor U, Salles FT, Grati M, Kachar B, Yengo CM. Intermolecular autophosphorylation regulates myosin IIIa activity and localization in parallel actin bundles. J Biol Chem. 2010; 285(46):35770–35782. [PubMed: 20826793]

Quintero OA, Unrath WC, Stevens SM Jr, Manor U, Kachar B, Yengo CM. Myosin 3A kinase activity is regulated by phosphorylation of the kinase domain activation loop. J Biol Chem. 2013; 288(52):37126–37137. [PubMed: 24214986]

Salles FT, Merritt RC Jr, Manor U, Dougherty GW, Sousa AD, Moore JE, Yengo CM, Dosé AC, Kachar B. Myosin IIIa boosts elongation of stereocilia by transporting espin 1 to the plus ends of actin filaments. Nat Cell Biol. 2009; 11(4):443–450. [PubMed: 19287378]

Schneider ME, Dosé AC, Salles FT, Chang W, Erickson FL, Burnside B, Kachar B. A new compartment at stereocilia tips defined by spatial and temporal patterns of myosin IIIa expression. J Neurosci. 2006; 26(40):10243–10252. [PubMed: 17021180]

Seiler C, Ben-David O, Sidi S, Hendrich O, Rusch A, Burnside B, Avraham KB, Nicolson T. Myosin VI is required for structural integrity of the apical surface of sensory hair cells in zebrafish. Dev Biol. 2004; 272(2):328–338. [PubMed: 15282151]

Self T, Sobe T, Copeland NG, Jenkins NA, Avraham KB, Steel KP. Role of myosin VI in the differentiation of cochlear hair cells. Dev Biol. 1999; 214(2):331–341. [PubMed: 10525338]

Senften M, Schwander M, Kazmierczak P, Lillo C, Shin JB, Hasson T, Géléoc GS, Gillespie PG, Williams D, Holt JR, Müller U. Physical and functional interaction between protocadherin 15 and myosin VIIa in mechanosensory hair cells. J Neurosci. 2006; 26(7):2060–2071. [PubMed: 16481439]

Shearer AE, Hildebrand MS, Sloan CM, Smith RJ. Deafness in the genomics era. Hear Res. 2011; 282(1-2):1–9. [PubMed: 22016077]

Sirmaci A, Edwards YJ, Akay H, Tekin M. Challenges in whole exome sequencing: an example from hereditary deafness. PLoS One. 2012; 7(2):e32000. [PubMed: 22363784]

Trivedi DV, Muretta JM, Swenson AM, Thomas DD, Yengo CM. Magnesium impacts myosin V motor activity by altering key conformational changes in the mechanochemical cycle. Biochemistry. 2013; 52(27):4710–4722. [PubMed: 23725637]

Walsh T, Walsh V, Vreugde S, Hertzano R, Shahin H, Haika S, Lee MK, Kanaan M, King MC, Avraham KB. From flies' eyes to our ears: mutations in a human class III myosin cause progressive nonsyndromic hearing loss DFNB30. Proc Natl Acad Sci U S A. 2002; 99(11):7518–7523. [PubMed: 12032315]

Walsh T, Pierce SB, Lenz DR, Brownstein Z, Dagan-Rosenfeld O, Shahin H, Roeb W, McCarthy S, Nord AS, Gordon CR, Ben-Neriah Z, Sebat J, Kanaan M, Lee MK, Frydman M, King MC,

Avraham KB. Genomic duplication and overexpression of TJP2/ZO-2 leads to altered expression of apoptosis genes in progressive nonsyndromic hearing loss DFNA51. Am J Hum Genet. 2010; 87(1):101–109. [PubMed: 20602916]

Walsh VL, Raviv D, Dror AA, Shahin H, Walsh T, Kanaan MN, Avraham KB, King MC. A mouse model for human hearing loss DFNB30 due to loss of function of myosin IIIA. Mamm Genome. 2011; 22(3-4):170–177. [PubMed: 21165622]

Yan D, Zhu Y, Walsh T, Xie D, Yuan H, Sirmaci A, Fujikawa T, Wong AC, Loh TL, Du L, Grati M, Vlajkovic SM, Blanton S, Ryan AF, Chen ZY, Thorne PR, Kachar B, Tekin M, Zhao HB, Housley GD, King MC, Liu XZ. Mutation of the ATP-gated P2X(2) receptor leads to progressive hearing loss and increased susceptibility to noise. Proc Natl Acad Sci U S A. 2013; 110(6):2228–2233. [PubMed: 23345450]

Yasunaga S, Grati M, Cohen-Salmon M, El-Amraoui A, Mustapha M, Salem N, El-Zir E, Loiselet J, Petit C. A mutation in OTOF, encoding otoferlin, a FER-1-like protein, causes DFNB9, a nonsyndromic form of deafness. Nat Genet. 1999; 21(4):363–369. [PubMed: 10192385]

Yengo CM, Takagi Y, Sellers JR. Temperature dependent measurements reveal similarities between muscle and non-muscle myosin motility. J Muscle Res Cell Motil. 2012; 33(6):385–394. [PubMed: 22930330]

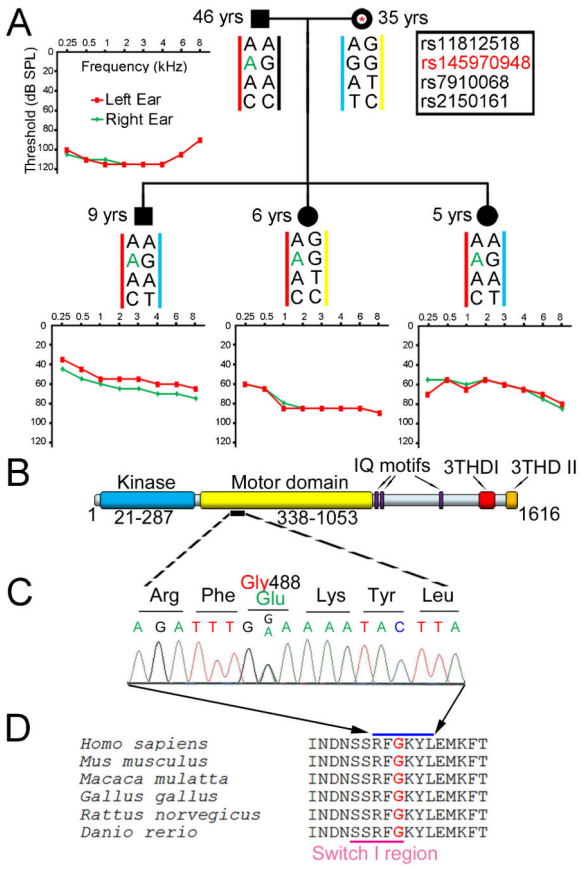

Figure 1.

Identification of a novel dominant mutation in *MYO3A* causing deafness in an African-American family. ***A***, African-American family tree composed of parents and 3 deaf children. Pure-tone audiometry of both left (red trace) and right (green trace) ears of each member. SNPs rs11812518, rs145970949 (*MYO3A* c.1463G>A), rs7910068 and rs2150161 genotype of each member was determined by Sanger sequencing, and their respective haplotypes was extrapolated by segregation analysis. The same paternal haplotype containing the only nucleic variation c.1463G>A (NC_000010.10:g.26377235G>A) in *MYO3A* identified by whole exome sequencing causing p.Gly488Glu mutation transmitted to all three children. The younger daughter and the son inherited a common maternal haplotype, while the older daughter inherited a distinct haplotype, reflecting random maternal *MYO3A* allele transmission. Although the mother suffered from moderately severe hearing-loss, the etiology of her deafness is unknown. ***B***, Domain representation of MYO3A pinpointing to the first switch region in the motor-head domain. ***C***, Electrofluorogram of *MYO3A* genomic sequence of an affected child showing heterozygous nucleic substitution c.1463G>A, which causes amino acid substitution p.Gly488Glu.***D***, Substitution p.Gly488Glu occurs in switch region I of the motor-head domain of MYO3A which is highly conserved from human to zebrafish.

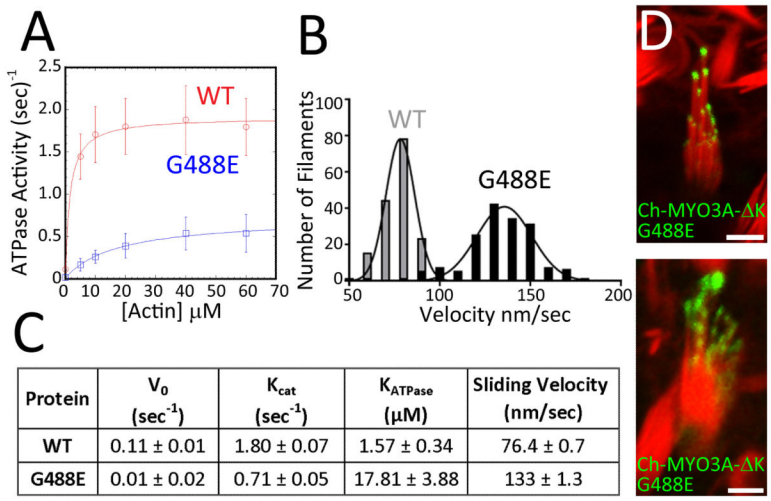

C

Protein	V_0 (sec^{-1})	K_{cat} (sec^{-1})	K_{ATPase} (µM)	Sliding Velocity (nm/sec)
WT	0.11 ± 0.01	1.80 ± 0.07	1.57 ± 0.34	76.4 ± 0.7
G488E	0.01 ± 0.02	0.71 ± 0.05	17.81 ± 3.88	133 ± 1.3

Figure 2.

Biochemical characterization and targeting in hair cells of p.Gly488Glu mutant MYO3A. ***A***, Actin-activated ATPase activity. The ATPase activity was plotted as a function of actin concentration and the data were fit to a hyperbolic function to determine maximum ATPase activity (k_{cat}) and actin concentration at which ATPase is one-half maximal (K_{ATPase}). Error bars represent standard errors from 3 separate protein preparations. ***B***, *In vitro* motility assay. The ensemble based movement of actin filaments generated by wild-type and p.Gly488Glu MYO3A was compared. The average sliding velocities (n=150 filaments) were fit to a Gaussian function demonstrating that p.Gly488Glu mutant MYO3A generates faster actin sliding velocities than wild-type MYO3A. ***C***, Summary of kinetic parameters extrapolated from actin-activated ATPase activity and *in vitro* motility assays on wild type and p.Gly488Glu mutant MYO3A. ***D***, Expression of p.Gly488Glu mutant Ch-MYO3A-ΔK (red channel switched into green color for better visualization) in P2 inner ear organotypic culture vestibular hair cells showing stereocilia (red) tip localization; actin is labelled using phalloidin-Alexafluor. Scale bar: 10 µm.

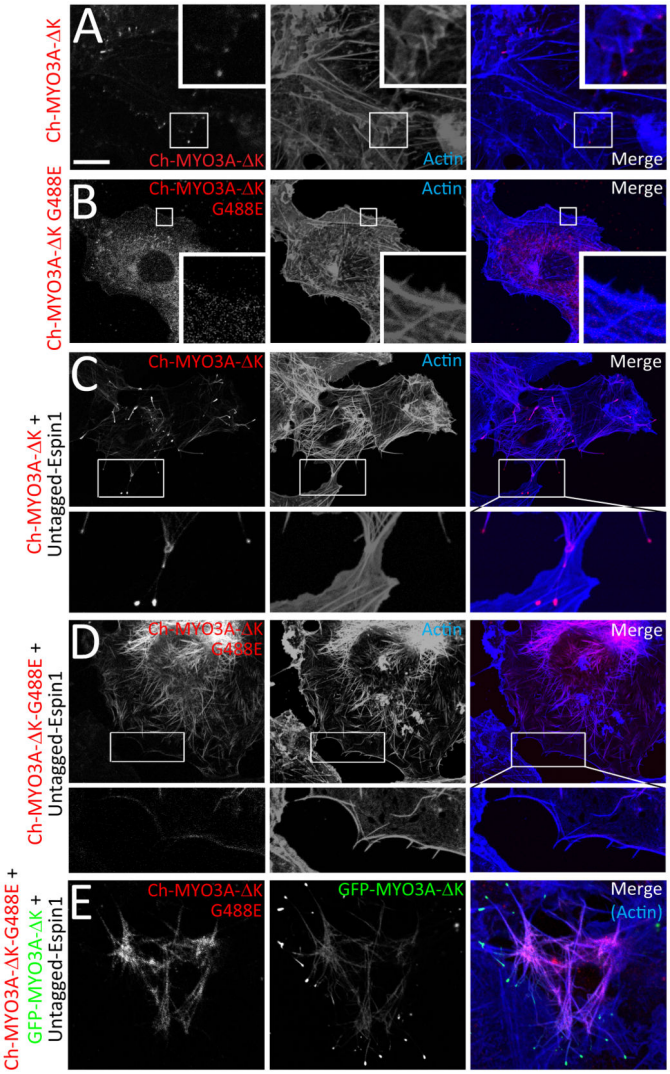

Figure 3.

Characterization of p.Gly488Glu mutation in COS7 cells. (***A***-***D***) Confocal images of COS7 cells expressing wild type Ch-MYO3A-ΔK (red in ***A***, ***C***) or p.Gly488Glu mutant Ch-MYO3A-ΔK (red in ***B***, ***D***) alone (***A***, ***B***) or together with untagged Espin1 (***C***, ***D***). A zoom-in view on filopodia of a highlighted region in each panel is also shown. ***E***, Confocal images of COS7 cells co-expressing p.Gly488Glu mutant Ch-MYO3A-ΔK and GFP-MYO3A-ΔK with Espin1. Scale bar: 10 μm.